A theoretical study of electronic factors affecting hydroxylation by model ferryl complexes of cytochrome P-450 and horseradish peroxidase

Michael Filatov, Nathan Harris and Sason Shaik *

Department of Chemistry and The Lise Meitner-Minerva Center for Computational Quantum Chemistry, The Hebrew University, 91904 Jerusalem, Israel

Received (in Cambridge) 1st December 1998, Accepted 15th January 1999

Density functional theory (DFT) is used to study model ferryl species of cytochrome P-450 and horseradish peroxidase (HRP), as well as of the product complex due to oxidation of H_2 by the P-450 species (**1**–**4** and **7**). The ferryl species studied include neutral and cation radical states of the porphyrin, as well as high- and low-spin situations. A few issues are addressed concerning the mechanism of alkane hydroxylation, and theoretical support is provided for: (i) the contention that spin inversion occurs along the reaction path, (ii) that the cation radical state of the porphyrin is an essential feature required to accommodate an excess electron from the ferryl moiety and thereby stabilize the ground state of the hydroxylation product, and (iii) that the donor property of the proximal ligand has a significant influence on the energy of the ferryl-to-ring charge-transfer states which are essential to convert the reactant state to the hydroxylation product state. In this sense, our study sheds some light on the difference between the oxidized and reduced HRP forms, HRP(I) and HRP(II), and suggests that the combination of a cation radical porphyrin state and a good π-donor proximal ligand like thiolate, could be the underlying reason for the potent hydroxylation ability of the P-450 ferryl-complex.

Introduction

Cytochrome P-450 and horseradish peroxidase (HRP) represent two families of heme enzymes that are used in nature as a means of biological oxidation of toxic compounds.[1–5] The active species in these enzyme families is considered[1,3–5] to be the iron-oxo compound, shown in Scheme 1, in which the ferryl group $Fe^{IV}O$ is embedded into the protoporphyrin IX ring. While in P-450 oxidation there exists evidence[6,7] for an additional active species (*e.g.*, peroxo-complex), attention here will be restricted to the ferryl-complex. An interesting feature of the ferryl moiety is its high-spin O_2-type bonding with two triplet electrons occupying the π*-orbitals of FeO.[1–5] The P-450 and HRP active species differ in the identity of the sixth ligand, the so called 'proximal ligand', which is a nitrogen from the imidazole of a histidine residue for the HRP species and a negatively charged sulfur moiety of a cysteine residue in the P-450 species. Other members of these families are secondary-amine monooxygenase (SAMO) which is analogous to HRP, and chloroperoxidase (CPO) which is analogous to P-450, and so on.

The ferryl species of HRP (Scheme 1) appears in two forms, HRP(I) and HRP(II), which differ in the oxidation state of the porphyrin ring. Thus, in HRP(I) the porphyrin moiety is a cation radical porphyrin, while in the HRP(II) form, the porphyrin is closed-shell.[4,5] The active form of P-450 has not been isolated, but model studies[1,3,4,8] suggest that it is analogous to HRP(I) with a cation radical state for the porphyrin. The species with the cation radical situation are typified by a high-spin state in which the odd electron of the cation radical is ferromagnetically coupled to the triplet electrons of the ferryl moiety ($S = 3/2$, *i.e.*, a quartet state).[1–5] In a few studies[9] it was shown that the cation radical state is an essential ingredient, in the absence of which the oxygen transfer capability of the ferryl species diminishes. This finding appears intriguing, since bare ferryl is capable of carrying out oxygen transfer reactions in the gas phase,[10] and one wonders what could be the precise difference between the nature of free ferryl and of the one embedded in a porphyrin ring. Thus, the 'hole' in the porphyrin ring appears to be a fundamental oxidative feature that requires elucidation.

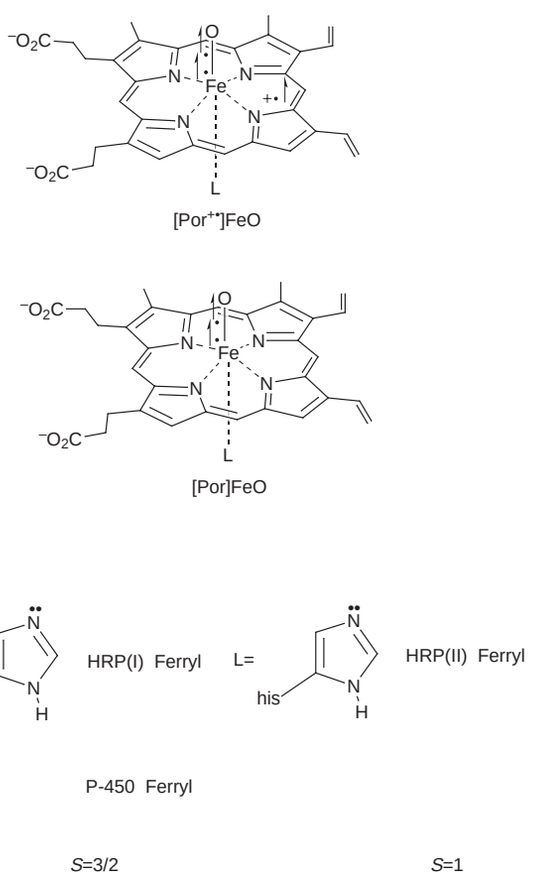

Scheme 1

Among the important oxidation reactions is the hydroxyl-

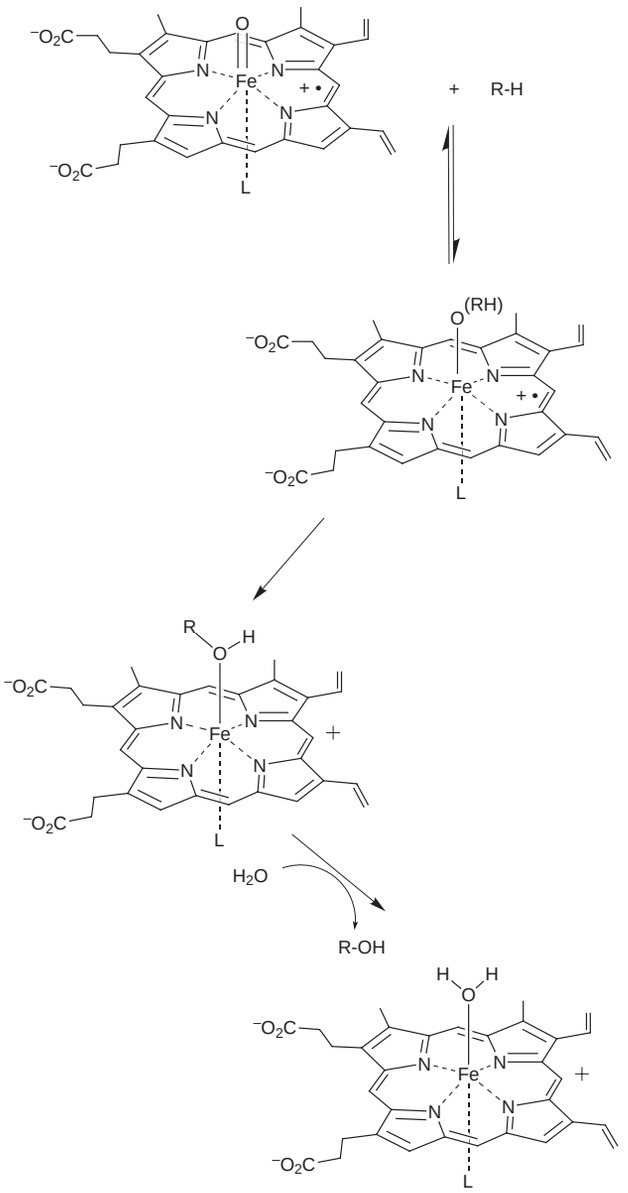

Scheme 2

ation of alkanes to alcohols, in Scheme 2. The net effect of the reaction is the insertion of the ferryl oxygen into the C–H bond to form the alcohol complex followed by regeneration of the resting state of the enzyme which is the iron–water complex. In this respect, P-450 is a very potent oxidant capable of hydroxylating even nonactivated C–H bonds of simple alkanes.[1,3] On the other hand, HRP(I) hydroxylates only activated C–H bonds, while HRP(II) is apparently not a hydroxylating agent; again implying a key role for the 'hole state' of the porphyrin.[9]

It has been proposed that the difference between HRP(I) and P-450 may originate in differences of accessibility of the iron center due to shielding by respective proteins.[1–3] Nevertheless, it is still important to ascertain whether or not any of the reactivity patterns are also associated with electronic factors due to the different proximal ligands of the two species. Indeed, it was proposed in numerous studies[1,3,8b,11] that the cysteinato proximal ligand plays a significant role in the 'O' insertion capability of P-450 into nonactivated C–H bonds. Generally speaking, electronic effects due to proximal ligands are well documented in epoxidation reactions by model compounds,[12] and hence the role of the proximal ligand is another intriguing issue which merits attention.

A third fundamental issue is concerned with the nature of the states which participate in the hydroxylation mechanism. In a

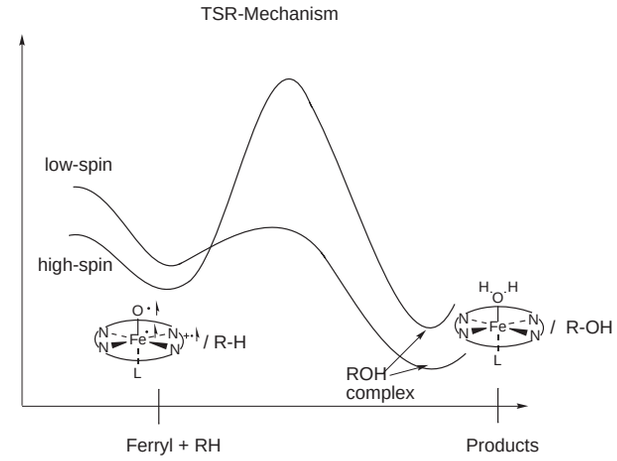

Fig. 1 Qualitative energy profiles following reference 15 showing a possible two-state-reactivity (TSR) situation for hydroxylation of alkane by P-450 ferryl complex. The TSR refers to the spin-state crossing along the reaction coordinate.

series of studies on the reactivity of bare ferryl, it was shown that the high-spin hydroxylation surface is typified by a high barrier and generates an addition adduct which is not very stable.[13] Consequently, the high-spin surface is crossed by a low-spin surface which is initially an excited state of the ferryl, and which is typified by low barriers and a stable hydroxylation adduct. The existing evidence in the area of P-450 hydroxylation suggests a similar mechanism in at least one case where spin state information is available for the hydroxylation product. Thus, whereas the ground state of the active species[1–5] is high-spin, the product-complex resulting from hydroxylation of camphor is low-spin.[14] Indeed, a hydroxylation mechanism based on a two-state-reactivity (TSR) paradigm has been recently proposed for P-450 hydroxylation,[15] in which a key role is played by the transitions between high- and low-spin potential energy surfaces of the reaction system, as shown in Fig. 1. All these pieces of evidence, taken together, indicate that even a minimalistic approach would require the consideration of two spin states of the ferryl species, for any hydroxylation mechanism.[4,6,16]

The above three fundamental issues form a broad topic which requires an equally extensive program before any satisfactory resolution of the problems can be achieved. As a first step we present in this paper density functional theoretical studies of various spin and state situations for model P-450 and HRP reactant species with closed-shell and radical-cationic porphyrin situations, as well as of a hydroxylation-product species (**1–4**, and **7** in Scheme 3 later). This paper provides supporting theoretical evidence for a TSR reactivity scenario in which the cation radical state of the porphyrin is required to stabilize the ground state of the hydroxylation product, and in which the proximal ligand affects the energy of the intramolecular charge-transfer states which fill the hole and eventually correlate to the hydroxylation product state.

Theoretical methods and strategy

Methods

Our method of choice is density functional theory (DFT), which has become a powerful tool for investigating transition metal compounds.[17] The calculations presented later have been done with the unrestricted Kohn–Sham method and the BP86 density functional[18] as implemented in the CADPAC5[19] suite of programs. This functional which includes nonlocal exchange and correlation corrections has already proven successful in the study of the various state and spin situations of an HRP complex and other ferryl complexes.[20] A basis set of double-zeta quality with polarization functions (DZVP2) especially opti-

mized for DFT calculations[21] was used on the metal, while for the coordination sphere of iron we used the 6-31G* basis,[22] and the STO-3G basis[22] on the C and H porphyrin atoms. Other studies performed by us on some of the species, with FT97[23] as well as BP86 with larger basis sets[24] gave virtually the same results, but were abandoned for reasons of computer time economy. All the structures were obtained *by full geometry optimization*, with the exception of a D_{4h} constraint of the porphyrin ring.

Below we describe the ground and excited state species which have been calculated, and provide necessary theoretical details for the calculation of the excited states using DFT.

Strategy

Model species. Scheme 3 shows, in **1**–**4**, models of the active species of P-450, HRP(I) and HRP(II), where the protoporphyrin substituents and proximal ligands have been simplified by necessity to save computer time and enable thereby the geometry optimization. Thus, the N-ligation of imidazole is simplified initially to NH_3 in **2**, and then to $H_2C{=}NH$ in **3**; the latter ligand has π-orbitals which can interact with the porphyrin in a manner at least analogous to imidazole. The cysteinato ligand of P-450 is simplified to HS^- in **4**. In view of the fact that the cysteinato moiety bears two electron attracting substituents (NH_3^+ and CO_2H), it was felt that HS^- which possesses a higher electron affinity can serve as a better model than CH_3S^-. The choice is not crucial for the present paper, though in general a judicious modeling of the ligand is important. Compound **1** serves as a reference in which the ferryl-complex is devoid of a proximal sixth ligand. All the species in **1**–**4** are studied in two oxidation states which will presumably give rise to closed-shell as well as cation radical porphyrin states. Furthermore, for all the species we also screened some excited states which may be relevant for the hydroxylation process.

Also shown in Scheme 3 are O_2 (**5**) and FeO^{2+} (**6**) which serve as bonding analogs for the ferryl moiety in the ferryl-complexes.[15] Note that FeO^{2+} in **6** has a formal oxidation state Fe^{IV} as in the porphyrin complexes.[1–5] Finally, in **7** we study the high- and low-spin states of the hydroxylation product of H_2 by the model P-450 active species.

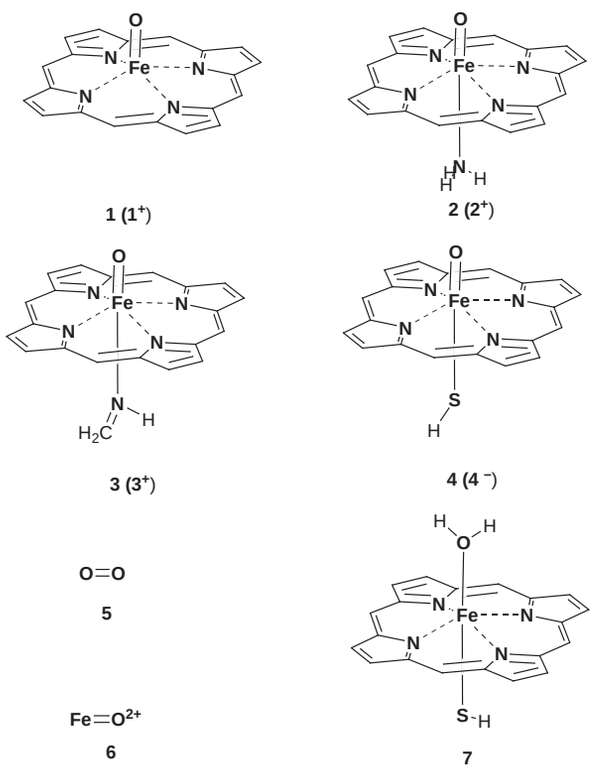

Scheme 3

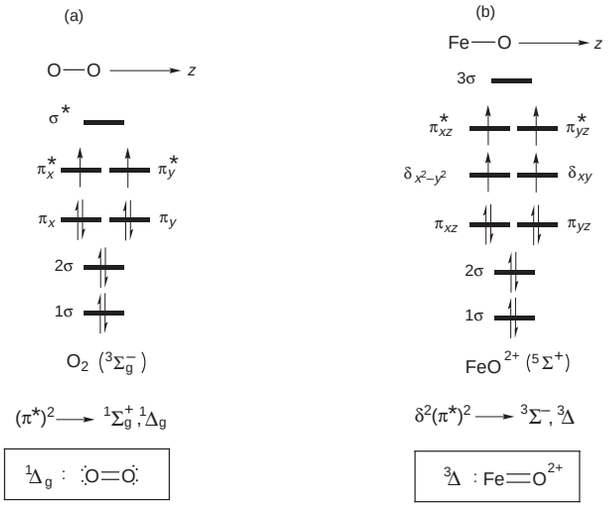

Fig. 2 Valence orbital energy diagrams and ground state configurations for O_2 (in a) and FeO^{2+} (in b). Below each diagram are shown the excited states nascent by distributing electrons among the highest lying π* and/or δ orbitals. The boxes depict the doubly bonded excited state Δ-type species.

Excited state calculations. Two types of excited states which are likely to have a role[15] along the hydroxylation path have been calculated. These are: the O_2-like excited states and the internal charge-transfer states of the types ferryl-to-ring and ligand-to-ring. Our interest is primarily in the qualitative trends along the series of species **1**–**4**, and hence the correct symmetry assignment for these excited states is important to us.

Fig. 2 depicts the corresponding orbital energy diagrams for the high-spin states of O_2 and FeO^{2+}. Both species have states which are also eigenstates of the angular momentum operator. Since the unrestricted Kohn–Sham (UKS) method is not capable of producing states with the correct angular momentum, except for high-spin states, we applied the vector coupling scheme,[25] which enabled us to calculate the energy for the correct state symmetry from the single Kohn–Sham (KS) determinant energies. This scheme is approximate because it does not optimize orbitals for the respective states, and therefore its reliability is in a way after the fact. In this sense, it is pointed out that the scheme has been successfully applied to excited state calculations for various transition metal complexes and has demonstrated a good ability to predict the state energies as well as the corresponding structural parameters.[26] Unlike methods of annihilation[27] or projection[28] within the UKS approach, this scheme enables one to calculate multiplets with spatial degeneracies.[25] From the theoretical point of view, each KS determinant contributing into the energy of a multiplet state corresponds to a mixed-symmetry state which possesses a single determinant noninteracting reference.[29]

The equations for the vector coupling scheme are collected in the Appendix to this paper, while here we give a short description of these states. Thus, O_2 possesses a $^3\Sigma_g^-$ ground state and $^1\Delta_g/^1\Sigma_g^+$ excited states, all nascent from a $(\pi^*)^2$ electronic configuration [Fig. 2(a)]. Thus for example, as shown in Fig. 2(a) below the orbital diagram, the low lying $^1\Delta_g$ excited state contains the 'classical' doubly bonded O=O species, whereas the ground state is a triplet π-diradical, $^3\Sigma_g^-$.

The orbital diagram of FeO^{2+} in Fig. 2(b) shows the valence configuration $1\sigma^2 2\sigma^2\pi^4\delta^2(\pi^*)^2$ for the high-spin $^5\Sigma^+$ state. The corresponding O_2-like low-spin states are nascent from the same valence configuration $1\sigma^2 2\sigma^2\pi^4\delta^2(\pi^*)^2$ by electron reshuffling in the π*- and δ-orbitals. The $^3\Delta$ and the $^3\Sigma^-$ state derive from the high-spin $^5\Sigma^+$ state by realignment of the π* electrons, while keeping the δ-electrons in a high-spin relation.

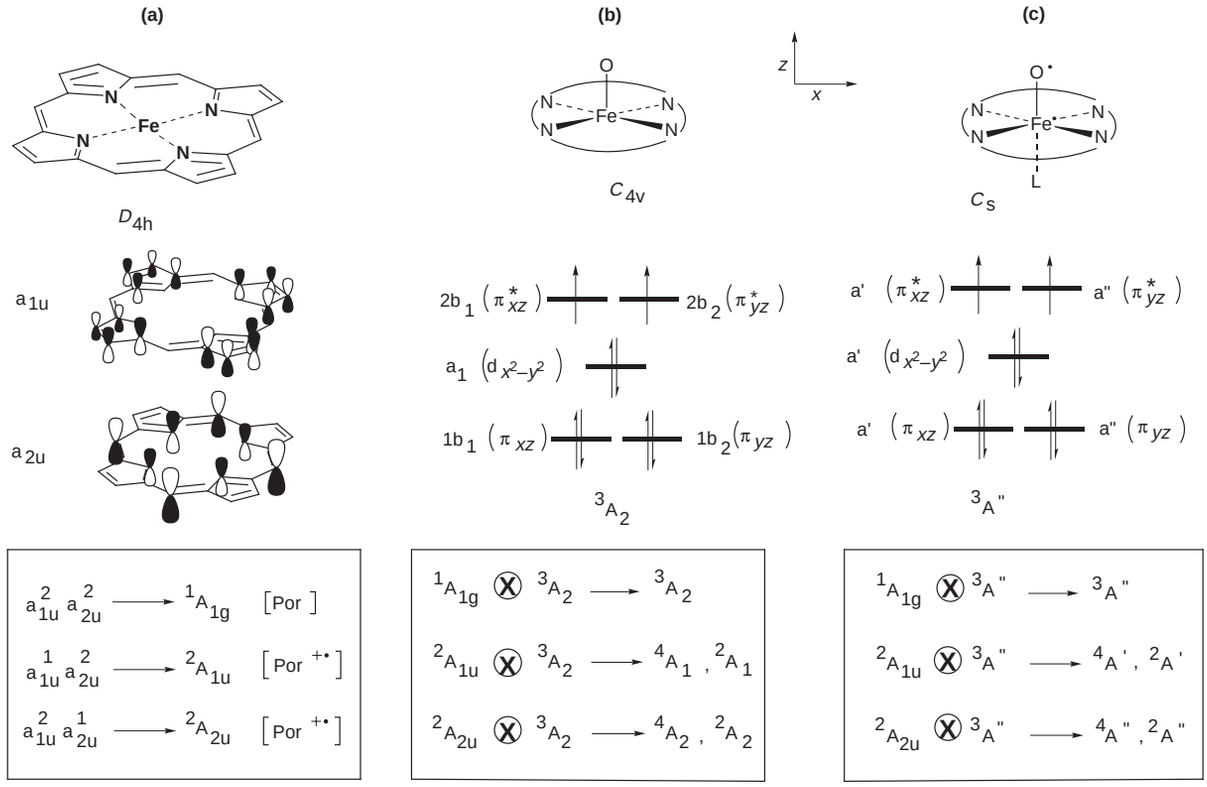

Fig. 3 (a) The a_{1u} and a_{2u}-type orbitals, and the state symmetries for the closed-shell and cation radical situations of porphyrin. (b and c) The valence orbital diagram of the ferryl moiety in C_{4v} and C_s point groups. In the boxes are shown the combined state symmetries of the ferryl-porphyrin complex. The cation radical porphyrin generates both high- and low-spin states due to different spin coupling as shown in Scheme 4.

Thus, the $^3\Delta$ state is an analog of the $^1\Delta_g$ state of O_2 with an Fe=O double bond, while $^3\Sigma^-$ is an analog of the $^1\Sigma_g^+$ state of O_2.

The orbital schemes for the ferryl complexes are shown in Fig. 3. The porphyrin frontier orbitals which belong to the a_{2u} and a_{1u} representations in the D_{4h} point group[20] are shown in (a) along with the local symmetry of the porphyrin state for the closed-shell and the two potential cation radical situations. The ferryl orbitals are shown in (b) and (c) for the C_{4v} and C_s ligand fields pertaining to the model compounds **1**–**4** in the oxidized and reduced forms. The δ-orbitals of the ferryl group split in the ligand field and only the lower lying $d_{x^2-y^2}$ is occupied with two electrons. The π*-antibonding orbitals remain degenerate in the C_{4v} ligand field and their splitting in the C_s ligand field is small. As such, these orbitals are occupied in (b) and (c) in a high-spin triplet situation, giving rise to $^3A_2$ and $^3A''$ state symmetry, which are analogs of the high-spin ground state of O_2.

Below the orbital diagrams in Fig. 3(b) and 3(c) we show the combined state symmetry for a closed-shell and cation radical porphyrin situations. Thus, the complexes with the closed-shell porphyrin remain $^3A_2$ and $^3A''$ for the C_{4v} and C_s ligand fields, respectively. In contrast, the states of the complexes with cation radical porphyrin become $^{2,4}A_{1,2}$, $^{2,4}A'$ and $^{2,4}A''$ depending on the ligand field symmetry (C_{4v} and C_s), the identity of the porphyrin's singly occupied orbital (a_{2u} or a_{1u}), and the mode of spin-coupling between the triplet ferryl module and the cation radical situation in the porphyrin. There are two modes of spin-coupling which are depicted in Scheme 4; mode (a) shows the high-spin quartet state which arises from the ferromagnetic coupling of the three electrons, while mode (b) shows the corresponding antiferromagnetic coupling.[20a,30–32] The ferromagnetic states have been computed for the ferryl complexes $\mathbf{2}^+$, $\mathbf{3}^+$ and **4** (Scheme 1), while the antiferromagnetic states have been computed only for the representative cases, $\mathbf{3}^+$ and **4**.

Two types of excited low-spin states implicated in the TSR reactivity of P-450[15] were computed for the ferryl complexes: (i) excited states of the ferryl moiety that involve a reshuffle of the π*-electrons as the corresponding O_2-like states in Fig. 2(a), and (ii) intramolecular electron transferred states which fill the 'hole' in the porphyrin, either from the π*-electrons of the ferryl group or from ligand orbitals.

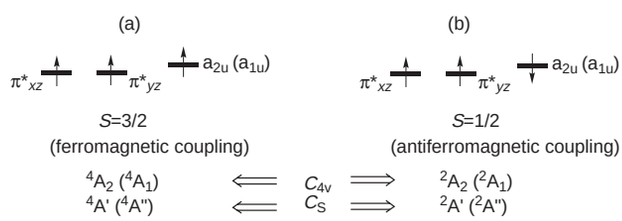

Scheme 4

Fig. 4 shows the O_2-like excitations along with their state symmetries in the C_{4v} and C_s ligand fields. In the C_{4v} ligand field, the $^1\Delta$-type states split into two states of B_1 and B_2 symmetry, while in the C_s ligand field these states become A′ and A″. The $^1\Sigma^+$-type states become either A_1 or A′. All these low-spin states are either singlets, for cases with closed-shell porphyrin, or doublets whenever the porphyrin has a cation radical situation.

Next, we turn to Figs. 5 and 6 to consider the intramolecular charge-transfer states which involve an electron transfer from either the ferryl moiety or the ligand into the singly occupied porphyrin orbital. These states are analyzed only for complexes with the cation radical porphyrin, since the compounds with a closed-shell ring have no appropriate low-lying orbital for accepting the transferred electron.

Fig. 5 shows the charge-transfer states arising by electron transfer from the ferryl π* orbitals to the singly occupied a_{2u} orbital, henceforth 'ferryl-to-ring charge-transfer states'. In the C_{4v} point group in (a) these excited states belong to the doubly degenerate representation (^2E). In the C_s group, in (b), this doubly degenerate charge-transfer state splits into $^2A'$ and $^2A''$ states nascent by electron transfer from the 2a″ and 2a′ π* orbitals into the a_{2u} type porphyrin orbital. In case (a) the ^2E

Table 1 Relative energetic, selected structural parameters, and spin densities in **1**–**4** and **6**

Entry	Species	Point group	State	Relative energy/ kcal mol^{-1}	FeN_{ring}/Å	FeO/Å	FeX/Å	Spin densities Fe	Spin densities O
FeO[Por$^{+\bullet}$] complexes									
1	**1**$^+$	C_{4v}	$^4A_1$	−2.8	2.014	1.638		1.26	0.79
			$^4A_2$	0.0	2.028	1.632		1.27	0.80
2	**2**$^+$	C_s	$^4A'$	+2.4	2.026	1.651	2.174	1.18	0.87
			$^4A''$	0.0	2.038	1.651	2.149	1.17	0.88
3	**3**$^+$	C_s	$^4A'$	+2.6	2.026	1.652	2.112	1.13	0.89
			$^4A''$[a]	0.0	2.038	1.653	2.083	1.11	0.89
4	**4**	C_s	$^4A'$	+9.7	2.028	1.689	2.433	1.21	0.86
			$^4A''$[b]	0.0	2.032	1.676	2.471	1.21	0.86
FeO[Por] complexes									
5	**1**	C_{4v}	$^3A_2$		2.024	1.643		1.30	0.75
6	**2**	C_s	$^3A''$		2.035	1.653	2.169	1.22	0.83
7	**3**	C_s	$^3A''$		2.035	1.652	2.095	1.16	0.85
8	**4**$^-$	C_s	$^3A''$		2.037	1.684	2.504	1.28	0.82
Bare ferryl									
9	**6**	$C_{\infty v}$	$^5\Sigma^+$			1.616		3.06	0.94

[a] The antiferromagnetic state for **3**$^+$ lies 11 cm^{-1} higher. [b] The antiferromagnetic state for **4** lies 31 cm^{-1} higher. In both cases, the state energies were calculated as in ref. 20*a*.

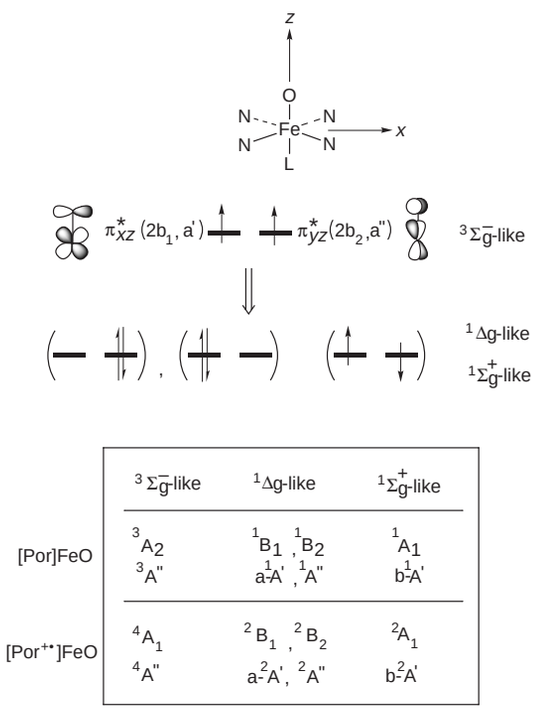

Fig. 4 O_2-like low-spin excited states of the ferryl complex and their symmetry assignment in C_{4v} and C_s point groups.

state does not have a symmetry match with the O_2-like low-spin states (in Fig. 4), and the two state types cannot mix. In case (b), there is a symmetry match between the two state types, but the coupling matrix elements between the symmetry matched states are expected to be small since they involve overlap between the ferryl π*-orbitals and a_{2u} or a_{1u} orbitals of the cation radical porphyrin. Hence, the charge-transfer states have been assumed to be noninteracting with the O_2-like states in the parent ferryl-complex geometry. As such, in both symmetry point groups, C_{4v} and C_s, the charge-transfer states can be represented by single determinants. Due to what seem to be serious degeneracies in this energy range, the spin-unrestricted SCF-KS procedure does not converge to the desirable states. Hence, the energies of the 'ferryl-to-ring charge-transfer states' have been estimated nonself-consistently, computing the energies of single determinants constructed from the ground state eigenvectors. These charge-transfer excitation energies are no doubt overestimated, but are expected to yield qualitative trends on the effect of different proximal ligands.

Fig. 6 shows the charge-transfer states arising by electron transfer from the ligand out-of-plane type orbitals to the singly occupied 'a_{2u}' orbital, henceforth 'ligand-to-ring charge-transfer states'. When the ligand is HS^-, in (a), the electron is transferred from the p-lone pair orbital of sulfur, while when the ligand is $HN{=}CH_2$, in (b) the electron is transferred from the $\pi_{N=C}$ orbital. Ferromagnetic excited states as well as an antiferromagnetic excited state are expected, depending on the spin coupling between the odd electron on the ligand and the triplet electrons of the ferryl group. The 'ligand-to-ring charge-transfer states' are computed in a SCF-KS procedure.

Results

Ground state properties of oxidized and reduced ferryl complexes

Table 1 summarizes the ground state properties of **1**–**4** and **6**, while Fig. 7 provides additional structural data for the ground states of the ferryl-complexes.

Electronic structure of the ground states. The data in Table 1 show that in all the oxidized forms in entries (1)–(4), the ground state is a high-spin quartet state typified by a cation radical porphyrin coupled ferromagnetically with a triplet π-diradical ferryl group. The antiferromagnetic states lie slightly higher (see comments in the Table), and indicate a very small coupling of the ferryl to the porphyrin odd electrons.

In the absence of a proximal sixth ligand (entry 1), the ground state $^4A_1$ involves the porphyrin cation radical in the $^2A_{1u}$ situation, while in the presence of an axial sixth ligand the ground state $^4A''$ involves the $^2A_{2u}$ porphyrin cation radical state. These results are in accord with experimental data,[1–5] with DFT calculations[20] as well as with CASCCF[30] and other calculations ranging from iterative extended Hückel[31] to X-α[32] and UHF;[33] all of which indicate that in the sixth coordinated ferryl-complex the porphyrin has a hole in the a_{2u} orbital. Comparing the complexes **2**$^+$ and **3**$^+$ shows that better π-donation of the sixth ligand in the latter complex has a negligible effect on the ground state properties of these complexes.

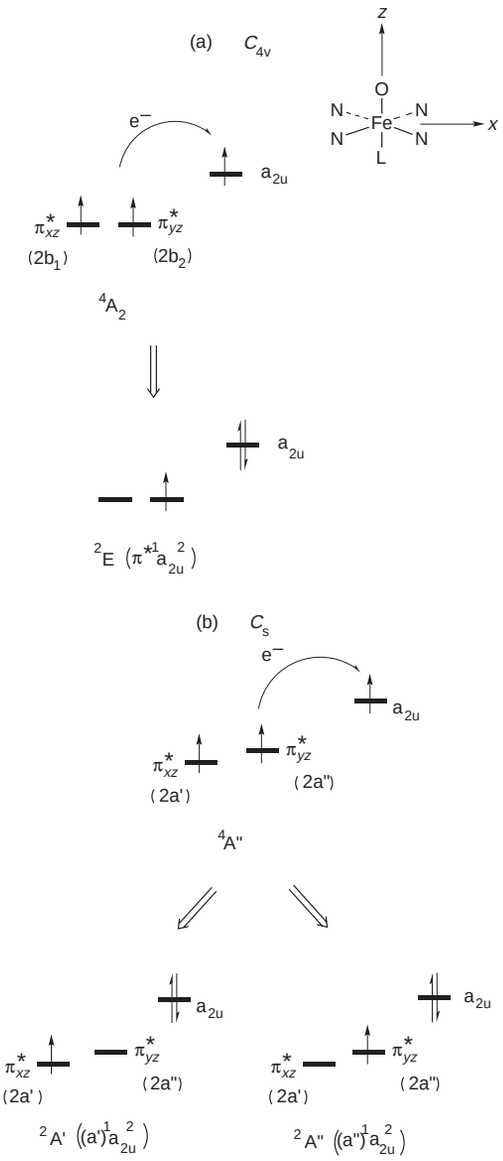

Fig. 5 Ferryl-to-ring charge-transfer states and their symmetry assignment in (a) C_{4v} point group, and in (b) C_s point group.

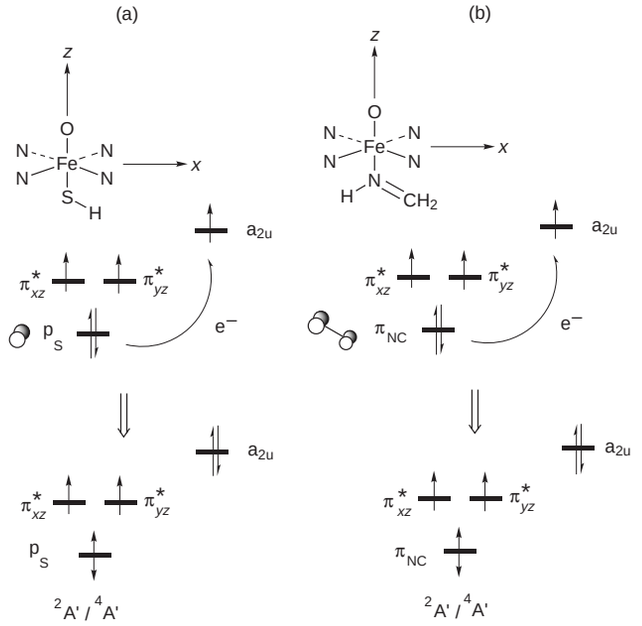

Fig. 6 Ligand-to-ring excited charge-transfer states for L = SH^- in (a) and L = NH=CH_2 in (b). The electron in the ligand orbital is drawn with a doubled-direction spin, such that the low- and high-spin situations correspond to antiferromagnetic and ferromagnetic spin coupling modes with that electron.

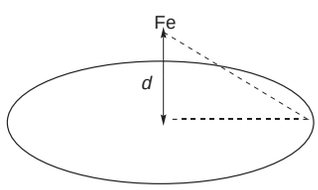

L	molecular charge	*d*/Å
none (**1**)	+ , 0	0.268, 0.305
NH_3 (**2**)	+ , 0	0.116, 0.149
H_2C=NH (**3**)	+ , 0	0.100, 0.129
SH^- (**4**)	0 , –	0.100, 0.075

Fig. 7 Fe-ring displacement parameters for the ferryl complexes (**1**–**4**) in the ground states of the oxidized and reduced forms.

In contrast, the thiolate ligand in **4** has a more significant effect on the state separation.

The ground states of the reduced forms, **1**–**4**$^-$, of the ferryl-complexes in entries (5)–(8), are all triplet states corresponding to O_2-like π-diradicals in accord with CASSCF[30] and experimental data.[31,34] Thus, as analyzed in Fig. 3 above, it is apparent from Table 1 that the oxidized form of the analogs of HRP(I) and P-450 ferryls (**1**$^+$–**4**) possesses two closely lying high-spin states with a 'hole' in the porphyrin ring and an O_2-like ferryl moiety, while in the reduced form analogs of HRP(II) there is one high-spin state associated with an O_2-like ferryl moiety.

Geometric features of the ground states. The optimized geometric parameters in Table 1 show that in the ferryl complexes, the Fe–O bond distance is in the range of 1.64–1.69 Å, well within the range of experimentally measured bond lengths for ferryl in active compounds: 1.604–1.68 Å.[1–5,20] For comparison we show in entry (9) that the calculated bond length for the $^5\Sigma^+$ ground state of the FeO^{2+} is 1.616 Å; also within the range of experimentally measured bond lengths for ferryls. The Fe^{IV}–S distance in **4** and **4**$^-$ is a bit long, but since the calculations reproduce a reasonable Fe^{III}–S bond length[11*b*] for the water complex (see later Fig. 8), we may consider that the BP86 result for the Fe^{IV}–S bond length in the ferryl complexes is reliable. In fact, all the optimized structural data for the ferryl complexes are in agreement with most models constructed from X-ray data and by restricted optimizations of the Fe–O bond.[4,11*b*,20,31–33,35] The complementary structural data in Fig. 7 show that without the sixth ligand the iron lies significantly above the porphyrin ring; by as much as 0.305 Å. The sixth ligand 'pulls' the iron back into the plane, albeit not completely. This trend is also in line with known experimental data.[1–5] There is no special ligand effect on this structural feature.[11*b*] The only structural effect exerted by the ligand is on the Fe–O bond, which as seen from Table 1 undergoes elongation for thiolate as a ligand. This latter effect is common to the oxidized and reduced ferryl-complexes, and provides some support for the 'push' effect discussed for thiolate ligands,[1,3,11*b–d*] and is generally expected from ligands which are good π-donors.[12*b*]

Finally, Table 1 shows also the computed spin-density distribution on Fe and O within the ferryl complexes. The spin density is almost equally distributed over the two atoms, in accord with the expected triplet π-diradical character of the Fe–O bond. The values of the spin densities are in accord with the recent DFT calculations of Kuramochi *et al.*[20*a*] performed with a larger basis set, with (SCC)X-α results,[32] as well as with the results of CASSCF calculations.[30]

Electronic structure of a product-complex state: a TSR scenario

Having ascertained the high-spin nature of the ground state, we turn to the product-complex state (**7**), which would correspond to the H_2 hydroxylation reaction nascent from the high-spin P-450 model compound (**4**). The results are depicted in Fig. 8 which shows the reactants, and the most stable structures for the high- as well as low-spin product complexes ($\mathbf{7}_{HS}$, $\mathbf{7}_{LS}$, $\mathbf{7}_{LS'}$).[36] The ground state of the complex is the low-spin doublet state of the product-complex ($\mathbf{7}_{LS}$); a result in accord with recent electron spin echo envelope modulation (ESEEM) spectroscopy of the water complex of P-450,[37] as well as with other experimental data of low-spin six coordinated Fe^{III} complexes which possess thiolate groups.[38] The plane of the water molecule and the porphyrin ring in $\mathbf{7}_{LS}$ are parallel, and this provides some extra stabilization due to internal hydrogen bonding between the protons of the water molecule and the negatively charged nitrogen atoms of the porphyrin. Indeed the two hydrogen bonded nitrogen atoms are found to carry a significantly higher negative charge than the other two. According to the ESEEM spectroscopic data[37] the water molecule is in an upright position. Our calculations show that this conformation shown in $\mathbf{7}_{LS'}$ is of higher energy. It was postulated[37] that the upright position is stabilized by hydrogen bonding with the protein which is in line with our interpretation that the parallel conformer $\mathbf{7}_{LS}$ is the most stable one due to the internal hydrogen bonding interactions. For both low-spin structures, the Fe–O bond lengths are well within the range of known experimental values for water molecules bonded to Fe.[14,35a] Other low-spin complexes of A′ symmetry were found to be significantly higher in energy and are not reported here. The corresponding high-spin quartet state $^4A''$ ($\mathbf{7}_{LS}$) is 13.6 kcal mol^{-1} less stable than the low-spin complex $\mathbf{7}_{LS}$ and has a virtually unbound water molecule. We conclude therefore that the ground state of the water-complex is $\mathbf{7}_{LS}/\mathbf{7}_{LS'}$ with $^2A''$ symmetry.

A rationale for the low-spin ground state of the water complex is provided in Scheme 5 using the upright water position for simplicity. The scheme shows the d^5 electronic configuration in the low- and the high-spin situations in (a) and (b). For a strong ligand field a low-spin occupation would be expected to possess lower energy than the corresponding high-spin complex, because the latter requires excitation of an electron from the d_{xz} orbital to the high lying $\sigma^*(d_{z^2})$ orbital. This electron occupation pattern results in a considerable Fe–O bond weakening and hence destabilization of the quartet high-spin product-complex, as evident from Fig. 8.

The above low-spin ground state of the product complex models experimental findings that the product complex of 5-hydroxycamphor with $P\text{-}450_{cam}$ is low-spin with a short Fe–O bond.[14,38a,39] This in turn shows that the hydroxylation process would generally be spin-nonconserving and involve crossover of high- and low-spin states along the reaction pathway, in accord with the recently proposed TSR paradigm[15] which is schematized in Fig. 1. Furthermore, as evident from Scheme 5, in both high- and low-spin product states the a_{2u} orbital is doubly occupied and the porphyrin ring is closed-shell; in contrast to the reactant ground state, where the a_{2u} orbital is singly occupied. Thus, there must be an internal electron transfer which fills the porphyrin's hole along the reaction pathway. The hole state then plays an essential role in the reaction.

The above results provide an incentive to look for excited low-spin states which may, on the one hand, fit the TSR concept and which, on the other hand, take into account the changes in the electronic structure from the reactant to the product state. These excited states are described below.

Table 2 O_2-like excitation energies (eV) of gas phase FeO^{2+} and O_2 excitation energies[a]

Entry	Transition	Excitation energy	
O_2 excitation energies			
1	$^1\Delta_g - ^3\Sigma_g^-$	1.025	
2	$^1\Sigma_g^+ - ^3\Sigma_g^-$	2.042	
FeO^{2+} excitation energies			
		r_{FeO} = 1.616 Å	r_{FeO} = 1.650 Å
3	$^3\Delta - ^5\Sigma^+$	1.172	1.113
4	$^3\Sigma^- - ^5\Sigma^+$	2.344	2.225

[a] See Fig. 2 for state definitions, and eqns. (1)–(4) in the Appendix.

O_2-Like excited states of FeO^{2+} and ferryl complexes

Table 2 collects the excitation energies for the species which serve as bonding models for the ferryl unit; the O_2 molecule, as well as the O_2-like excitations of FeO^{2+}. The calculations for FeO^{2+} have been carried out for the equilibrium bond length as well as for a stretched bond, 1.65 Å which corresponds to an

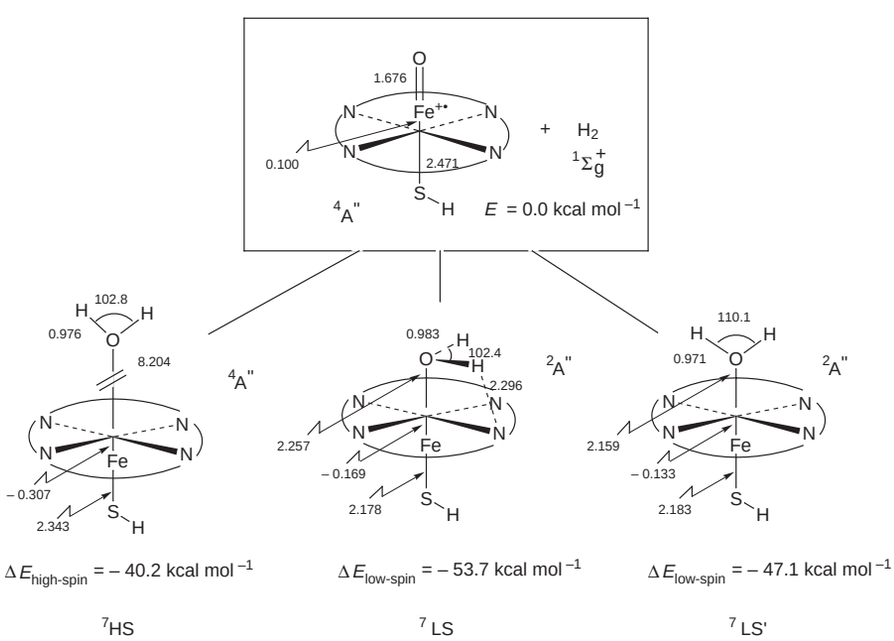

Fig. 8 Ground state of the P-450 ferryl complex model and the low- and high-spin product complexes for H_2 oxidation.

Table 3 Energies (eV) of the O_2-like excitations for ferryl-complexes[a]

Entry	Complex	Group	Ground state	Excited state/Excitation energy		
				$^2B_1$	$^2B_2$	$^2A_1$
1	$\mathbf{1}^+$	C_{4v}	$^4A_1$	0.698 (0.651[b])	0.883 (1.000[b])	1.581 (1.586[b])
				$^2A''$	a-$^2A'$	b-$^2A'$
2	$\mathbf{2}^+$	C_s	$^4A''$	0.689	0.916	1.606
3	$\mathbf{3}^+$	C_s	$^4A''$	0.659	0.866	1.544
4	**4**	C_s	$^4A''$	0.698	0.873	1.598
				$^1B_2$	$^1B_1$	$^1A_1$
5	**1**	C_{4v}	$^3A_2$	0.696	0.879	1.575
				$^2A''$	a-$^2A'$	b-$^2A'$
6	**2**	C_s	$^3A''$	0.689	0.904	1.593
7	**3**	C_s	$^3A''$	0.647	0.837	1.517
8	$\mathbf{4}^-$	C_s	$^3A''$	0.696	0.866	1.592

[a] See Fig. 4 for state definitions and eqns. (5)–(11) in the Appendix. [b] Datum obtained with the ROKS method.[41]

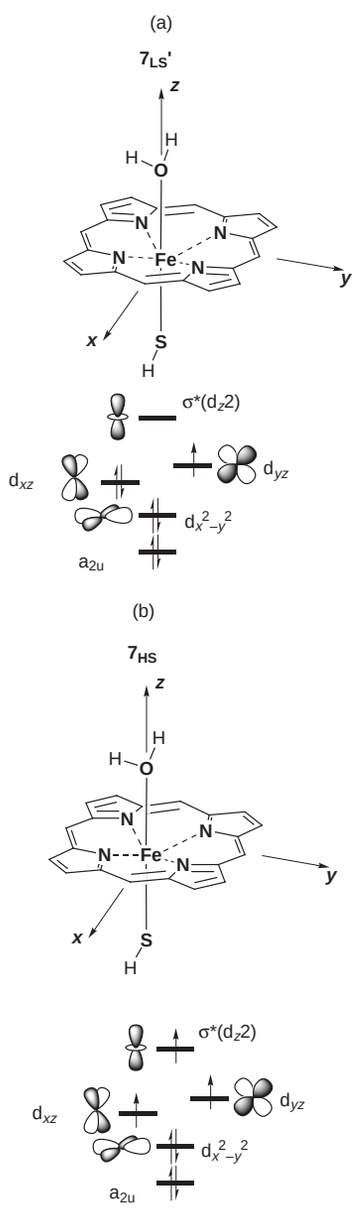

Scheme 5

average value in the ferryl-complexes (see Table 1). It is seen that the excitation energies (entries 1 and 2) from the high-spin ground state of O_2 to the corresponding low-spin excited states are in reasonable accord with experimental data.[40] The same results were obtained recently using the restricted open-shell Kohn–Sham (ROKS) method which employs orbital optimization,[41] thereby indicating that the vector coupling scheme[25] is quite reliable. The corresponding excitations of FeO^{2+} in entries 3 and 4 in Table 2 are of similar magnitudes, and are not very sensitive to the variations in the Fe–O bond length. The similarity between the states of the two species is indeed striking, albeit expected based on their common electronic origins (see Fig. 2).

The oxygen-like excitations in the ferryl-complexes **1**–**4** in their oxidized and reduced forms are presented in Table 3. The parenthetical values in entry 1 obtained with the ROKS method[41] show that the vector coupling scheme gives results within a few hundredth of eV from a result obtained by orbital optimization. The various states can be discussed with reference to Fig. 4. We recall that in the C_{4v} ligand field, in **1**, the Δ-type excited states split into two states of B_1 and B_2 symmetry, while in the C_s point group of **2**–**4**, these states are A″ and A′. The computed data in Table 3 show that the excitation energies of this type are quite insensitive to the nature of the axial ligand and state of the porphyrin, cation radical or closed-shell. The lowest excitation energy is *ca.* 30% lower than in the FeO^{2+} or oxygen molecules. These excitation energies are however in the same range as those calculated by CASPT2 for the bare FeO^+ molecule, which is another possible model for embedded ferryl: 0.5–0.8 eV.[13a] Hence, by analogy with the FeO^+ species, the low lying doublet state where the ferryl moiety is in a perfect pairing Fe=O situation, is energetically accessible and can become involved in the hydroxylation of alkanes *via* spin-state crossing.

Charge-transfer excited states of ferryl complexes

To identify low-spin excited states which are responsible for differences between the ferryl-complexes and account for the requisite internal electron transfer, we turn to the charge-transfer states, described in Figs. 5 and 6. The results of these calculations are given in Table 4; entries 1–4 provide the ferryl-to-ring excitations, while entries 5 and 6 list the ligand-to-ring excitations.

Inspecting entries 1–4, it is seen that, in the absence of the sixth axial ligand (in $\mathbf{1}^+$) the ferryl-to-ring charge-transfer excitation is very high, while a nitrogen ligand lowers the $^4A''\rightarrow{}^2A'$ excitation, the value still remains large. The most noticeable effect is produced by the thiolate ligand (**4**) which lowers the excitation energies to the two ferryl-to-ring charge-transfer states, with a larger effect on the $^2A'$ state. A similar effect of the proximal ligand is apparent from the ligand-to-ring charge-transfer excitations in entries 5 and 6 which show that the thiolate ligand gives rise to low lying states, in comparison with the π-donor ligand H_2C=NH (in $\mathbf{3}^+$). These qualitative trends are in general agreement with findings that the thiolate ligand produces low energy excited states[11d] in comparison with imidazole type ligands.

Table 4 Energies (eV) of the charge-transfer (CT) excitations

Entry	Complex	Group	Ground state	Excited state/Excitation energy	
Ferryl-to-ring CT state					
				^{2}E	
1	**1**$^+$	C_{4v}	$^4A_1$	4.839[a]	
				^{2}A′	^{2}A″
2	**2**$^+$	C_s	^{4}A″	4.804[b]	4.804[c]
3	**3**$^+$	C_s	^{4}A″	3.505[b]	4.873[c]
4	**4**	C_s	^{4}A″	2.182[b]	4.447[c]
Ligand-to-ring CT state					
				^{2}A′	^{4}A′
5	**3**$^+$	C_s	^{4}A″	6.219[d]	6.927[e]
6	**4**	C_s	^{4}A″	0.552[d]	0.897[e]

[a] Calculated as single determinant energy (see the Appendix for specifications of the orbitals) $E(^2E) = E(e_x a_{2u} \bar{a}_{2u})$. [b] Calculated as $E(^2A') = E(a' a_{2u} \bar{a}_{2u})$. [c] Calculated as $E(^2A'') = E(a'' a_{2u} \bar{a}_{2u})$. [d] Calculated as $E(^2A') = \frac{3}{2}E(a' a'' \bar{lp}_{a''}) - \frac{1}{2}E(a' a'' lp_{a''})$. [e] Calculated as $E(^4A') = E(a' a'' lp_{a''})$.

Discussion

The computational results make a case for a TSR reactivity[15] mechanism of hydroxylation, where quartet and doublet spin states intersect along the reaction path, and in which charge-transfer states play a role in preparing and stabilizing the product state, by filling the porphyrin 'hole'. The proximity of anti-ferromagnetic reactant states (Table 1) and the possibility that the reactant state exists in a dynamic mixture of high-spin and low-spin situations, will certainly assist the spin-state crossover along the reaction path[42] but will not altogether eliminate the requirement for spin–orbit coupling mediated transition from the high-spin ground state to the low-spin product-state. Let us then proceed to analyze some key issues projected by the results; the roles of the porphyrin 'hole' and of the excited states of the ferryl, as well as the effect of the proximal ligand through the charge-transfer states.

The role of the porphyrin 'hole'

The importance of the porphyrin 'hole' may be understood by reference to the electronic structure of the water-complex in Scheme 5, which shows that the 'a_{2u}' orbital is doubly occupied and the porphyrin is therefore closed-shell while the d-block of the metal contains five electrons in a $d_{x^2-y^2}{}^2 d_{xz}{}^2 d_{yz}{}^1$ formal configuration. Thus, imagine a hydroxylation process starting with a ferryl-complex that already possesses a closed-shell porphyrin, as *e.g.*, in the HRP(II) species. Since initially there is one additional electron, this would be required to populate in the hydroxylation-complex either the empty $\sigma^*(d_z2)$ orbital or the singly occupied d_{yz} orbital. The first option would have led to the population of a high lying orbital, while the second option would have required a closed-shell $d_{x^2-y^2}{}^2 d_{xz}{}^2 d_{yz}{}^2$ configuration (formal Fe^{II}) which is destabilized by virtue of electron–electron repulsion, and is unfavorable unless the ligand field is very strong. *Thus, the porphyrin's 'hole' serves as an electronic sink which stabilizes the hydroxylation product state.* This conclusion provides a theoretical rationale for the findings[9] that the compound (II)-type ferryl-complexes with the closed-shell porphyrin either do not exhibit an oxidative activity (see footnote 13 of ref. 9*a*) or are sluggish oxidants (ref. 9*b*). This is also in line with the fact that the HRP(II) compound does not participate in hydroxylation but rather in electron transfer *en route* to regeneration of the active species HRP(I).[2,3,5,11*b*]

The situation of the ferryl embedded in the porphyrin complex can be further compared with that of bare $Fe{-}O^+$[13] which performs hydroxylation without the presence of the porphyrin. Thus, bare FeO^+ with the dangling d-orbitals of the coordinatively unsaturated iron has a built-in electron sink,[13,43] whereas in the ferryl complex of *e.g.*, P-450, in which the iron is coordinatively saturated, *the sink has to be provided by the cation radical state of the porphyrin ligand.*

The role of the low-spin excited states of the ferryl-complex

The calculations focused on two excited state types which have a role along the hydroxylation path; the O_2-like excited states (Table 3) and the internal charge-transfer states (Table 4).

Consider first the O_2-like excited states. Initially in the high-spin ground state the ferryl unit has a half-filled valence shell and no low lying empty orbitals which can create bonding interactions with the substrate undergoing hydroxylation. In contrast, the low-spin states (especially the $^1\Delta$-types) possess a low lying empty orbital (π^*) which can interact with the substrate (RH) and lead to formation of the new O–H and O–R bonds. Thus, the role of O_2-like low-spin excited states is to activate the ferryl unit towards bond formation with the substrate.[13,15] The fact that these states are considerably lower than the corresponding states in the O_2 molecule itself (Table 2 *vs.* Table 3) implies also that ferryl-complexes will be more powerful oxidants than O_2.

The role of the internal charge-transfer states is to promote the electron reorganization that fills the porphyrin 'hole' along the reaction pathway. A more detailed orbital origin of the charge-transfer state can be defined by a simple electron count of the valence electrons of the reactant ferryl-complex and the product water-complex. Since the π and π^* orbitals of the ferryl unit have mixed Fe and O characters, all the corresponding electrons must be counted. This will require counting also the p-lone pair electrons of the water moiety in the product complex since this orbital mixes with the symmetry matched d-orbitals of the iron. Thus, initially the ferryl moiety involves eight electrons in the d/π block ($d^2\pi^4\pi^{*2}$, Fig. 3) and one electron in the 'a_{2u}' orbital. Finally, in the product complex, the Fe–O moiety contains seven electrons ($p_O{}^2 d_{x^2-y^2}{}^2 d_{xz}{}^2 d_{yz}{}^1$), while '$a_{2u}$' is doubly filled (Scheme 5). Thus, while the precise details of the charge-transfer may be complex, it is apparent that the ferryl moiety loses one electron to the porphyrin during the reaction. This in turn means that the ferryl-to-ring charge-transfer states participate in the internal electron transfer which occurs during the reaction. A simple rationale for this internal reorganization is *that in order for the ferryl oxygen to form two new bonds during the hydroxylation, and at the same time retain one Fe–O bond, one electron must be lost from the bonding block of the ferryl moiety and relayed by internal charge-transfer to the 'hole' in the porphyrin.*

It is important to recognize that along the reaction coordinate the charge-transfer states and the O_2-like excited states will mix with each other until correlation is achieved to the product state. Thus, it is the combination of the excited states which will promote the bonding reorganization required to transform the reactant state to the product state.

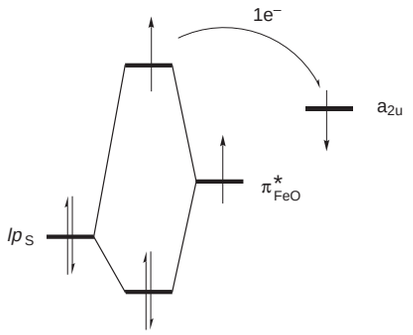

Fig. 9 The ligand assisted mechanism of internal electron transfer from the ferryl to the porphyrin ring along the hydroxylation pathway. The lone-pair orbital (*lp*) of the sulfur ligand mixes with the π* orbital of the ferryl. The electron in the antibonding combination orbital eventually fills the singly occupied a_{2u} orbital of the porphyrin.

The effect of the proximal ligand

The lower the energy of the state combination which correlates to the product state along the reaction pathway, the lower would be the crossing point between the quartet and doublet states (see Fig. 1) and the smaller the barrier for the process is likely to be. In this sense, it is apparent that while the O_2-like states (Table 3) are unaffected by the ligand, in contrast the charge-transfer states (Table 4) exhibit a significant dependence on the identity of the proximal ligand; the sulfur ligand being considerably more effective than the nitrogen ligands. Let us therefore discuss the possible pathways along which the proximal ligand effect may be expressed.

Inspection of Fig. 8 shows that the low-spin product state possesses $^2A''$ symmetry. Tables 3 and 4 show that there exist two sets of O_2-like and charge-transfer excited states with $^2A'$ and $^2A''$ symmetries. It is apparent therefore that it is the $^2A''$ combination of O_2-like and charge-transfer states which will eventually correlate to the product state. Nevertheless, the proximal ligand effect depends on the question of whether or not the hydroxylation reaction path conserves a plane of symmetry, *i.e.*, if all the structures along the path belong to the C_s point group.

If the reaction path conserves C_s symmetry, only the $^2A''$ states will affect reactivity. As seen by comparing entries 3 and 4 in Table 4, the SH^- ligand stabilizes the $^2A''$ charge-transfer state by *ca.* 0.4 eV in comparison with the CH_2=NH ligand. Such a pathway will exhibit a moderate effect of the proximal ligand making the thiolate-ferryl complex more reactive than its nitrogen-base alternative. If however, the reaction path does not conserve any symmetry, this will lead to the mixing of all the charge-transfer states, and since the $^2A'$ charge-transfer state (entries 4 *vs.* 3, and 6 *vs.* 5) is very strongly affected by the identity of the ligand, we may anticipate a much more pronounced ligand effect on reactivity. Thus, a ligand effect is expected irrespective of the reaction path symmetry, and the thiolate ligand should exert a more pronounced effect on the hydroxylation mechanism compared with the nitrogen-based ligand.

Fig. 9 shows an orbital interaction which accounts for the proximal ligand effect of the SH^- ligand. Sulfur has two lone-pair orbitals (a′ and a″ in C_s point group symmetry), and each one of them can mix with the symmetry matched singly occupied π* orbital of the ferryl unit, and form bonding and antibonding combinations, the latter made primarily of the π*(FeO) orbital. The mixing depends on the Fe–S distance, which is seen from Fig. 8 to undergo significant shortening (2.471→2.18 Å) with concomitant pulling of Fe toward the sulfur from the position above the porphyrin (+0.100 Å) to the position below it (−0.169 Å/−0.133 Å for $\mathbf{7}_{LS}$ and $\mathbf{7}_{LS'}$ respectively). Clearly, then, as the Fe–S bond gets shorter along the reaction path, the orbital mixing increases and the antibonding orbital combination will rise up to a point where it can depopulate its electron into the a_{2u} orbital of the porphyrin. The net effect is a significant stabilization of the system along the reaction coordinate. It follows therefore that the thiolate ligand stabilizes the charge-transfer state which is required to assist the transformation of reactants to products by providing a donor orbital that can mix with the ferryl π* orbitals and cause them to shift an electron to the porphyrin 'hole'.[44] The nitrogen base ligand HN=CH_2 has in comparison a $\pi_{N=C}$ orbital which is significantly lower than the thiolate lone-pair orbitals, and therefore HN=CH_2 has an ineffective orbital interaction and high lying charge-transfer states. Thus, it is here in the charge-transfer excitation that we see the impact of the proximal ligand which distinguishes the P-450 species (**4**) from the HRP(I) species ($\mathbf{3}^+$). Similar explanations were given before[11b,c] to account for this difference and the associated 'push' effect[1,3] of the proximal thiolate ligands. This electronic effect can be moderate to significant depending on whether or not the reaction path conserves C_s symmetry. Moreover, the proximal ligand effect is associated with the presence of the porphyrin hole, and as such the reduced ferryl complexes like HRP(II) and type (II)-ferryls would not be expected to exhibit a pronounced proximal ligand effect.

Summary and conclusions

Three fundamental issues were raised at the outset concerning the reactivity patterns of model ferryl-complexes of P-450 and HRP(I)/HRP(II) species (**1**–**4** in Scheme 3). What is the role of the cation radical state of the porphyrin in P-450 and type (I)-ferryl complexes? What is the effect of the proximal axial ligand in these complexes? And whether there occurs indeed a spin-state crossing during their hydroxylation reactions, as postulated in reference 15? Our DFT study and theoretical analysis provide insight into these problems and demonstrate their intimate link.

The calculations for P-450 and HRP(I)/HRP(II) species (**1**–**4** in Scheme 3) reveal that all the ferryl-complex models possess a high-spin ground state, in which triplet ferryl-electrons are ferromagnetically coupled to a porphyrin electron in a singly occupied orbital (a_{2u}) of the porphyrin cation radical. At the same time, the product state generated by P-450 oxidation of H_2 (**7** in Scheme 3) is in a low-spin doublet state. Thus, a case is made for a two-state-reactivity (TSR)[15] for P-450 alkane hydroxylation, where the initial high-spin surface is crossed by a low-spin surface along the reaction pathway.

The low-spin surface which eventually correlates to the product state is influenced by an internal charge-transfer state in which a ferryl π* electron is relayed into the singly occupied orbital (a_{2u}) of the porphyrin cation radical. This is mediated by the interaction of the ferryl moiety with both the proximal ligand and the substrate, along the hydroxylation pathway. Thus, the study provides supporting theoretical evidence that *the cation radical state of the porphyrin is an essential ingredient required to accept the relayed electron and stabilize thereby the ground state of the hydroxylation product, and that the donor property of the proximal ligand has a significant influence on the energy of the ferryl-to-ring charge-transfer states which are essential to convert the reactant state to the hydroxylation product state*. Thus, the role of the 'hole' state, the effect of the proximal ligand and the TSR aspect are all linked. In this sense, our study sheds some light on the difference between HRP(I) and HRP(II) or in general between type (I) and type (II) ferryls,[9] as well as on the effect of the proximal ligand.[12] One would expect that type (II)-ferryls which lack the porphyrin 'hole' will react generally slower than type (I) complexes, and will exhibit entirely different axial ligand effects.

The present results must eventually be complemented by further quantum-chemical calculations which can elucidate the full mechanistic details of the hydroxylation by ferryl-

porphyrins especially with regard to the transition states. Such studies are in progress.

Finally, the study provides a few intriguing features which merit attention in future studies. One is concerned with the ligand-to-ring charge-transfer states in the P-450 ferryl-complexes. It is apparent from Table 4 (entries 5 and 6) that these states are very low lying for the SH^- ligand, and this is no doubt related to the high lying donor orbital (a″) of sulfur.[45] It is reasonable to expect that in some thiolate derivatives the ground state of the ferryl-complex will involve a triplet ferryl coupled to a sulfur radical, like the charge-transfer states in Table 4 (entries 5 and 6). Trautwein *et al.*[32] have indeed reported such a high-spin ground state for the CH_3S^- ligand. In such an event, the 'hole' state shifts from the porphyrin to the proximal ligand and it plays a similar role to the porphyrin 'hole'. Our calculations (Table 4, entry 6) however show that the ground state for this situation is more likely to be a low-spin state ^{2}A″. Should this low-spin ground state be a common situation then the reactivity of thiolate derivatives will not follow TSR and will be distinct among the ferryl-complexes. The second intriguing feature is concerned with the dense manifold of ground states, which is exhibited in Table 1. Thus, within a range of a few kcal mol^{-1}, each ferryl complex possesses two different high-spin ferromagnetic states (*e.g.*, ^{4}A′ and ^{4}A″) and two antiferromagnetic twins. The oxidation process with background dynamics of all these states is a challenging problem to decipher. The loss of the Fe–O bond in the high-spin suggests that the high-spin and low-spin pathways will be differently affected by the protein environment. Finally, the movement of the proximal ligand, exemplified by the shortening of the Fe–S bond during the reaction (2.471→2.18 Å) suggests a significant role for the protein pocket which provides the proximal ligand group.

Acknowledgements

This research is supported by the WV Stiftung and G.I.F. (The German-Israeli Foundation).

Appendix

The Appendix provides expressions used in applying the vector coupling scheme[25] to the excited states of the various species.

Eqns. (1) and (2) were used to calculate the excited state energies for O_2 from the corresponding Kohn–Sham determinants (Table 2). Here the π* orbitals refer to the real Cartesian orbitals in the *x* or *y* direction perpendicular to the molecular axis. With these equations, the low-spin excited states acquire the correct electronic symmetry.

$$E(^1\Delta_g) = \tfrac{1}{2}[E(\pi_x^*\bar{\pi}_y^*) + E(\pi_x^*\bar{\pi}_x^*)] \quad (1)$$

$$E(^1\Sigma_g^-) = E(\pi_x^*\bar{\pi}_y^*) + E(\pi_x^*\bar{\pi}_x^*) - E(\pi_x^*\pi_y^*) \quad (2)$$

The corresponding state energies for FeO^{2+} are calculated (Table 2) using eqns. (3) and (4), where δ_x corresponds to the $d_{x^2-y^2}$ δ-type orbital and δ_y to d_{xy}.

$$E(^3\Delta) = \tfrac{1}{2}[E(\delta_x\delta_y\pi_x^*\bar{\pi}_y^*) + E(\delta_x\delta_y\pi_x^*\bar{\pi}_x^*)] \quad (3)$$

$$E(^3\Sigma^-) = 2E(^3\Delta) - E(^5\Sigma^+) \quad (4)$$

The ferryl states in C_{4v} and C_s groups (Fig. 3) are very similar and their energies (Table 3) can be expressed *via* single determinant energies as given in eqns. (5)–(11).

$$E(^3A_2) = E(e_xe_y); \quad e_x = \pi_x^*, e_y = \pi_y^* \quad (5)$$

$$E(^1B_2) = 2E(e_x\bar{e}_y) - E(^3A_2) \quad (6)$$

$$E(^1B_1) = E(e_x\bar{e}_x) + E(e_x\bar{e}_y) - E(^1B_2) \quad (7)$$

$$E(^1A_1) = E(^1B_2) + E(^1B_1) - E(^3A_2) \quad (8)$$

$$E(^3A'') = E(a'a''); \quad a' = \pi_x^*, a'' = \pi_y^* \quad (9)$$

$$E(^1A'') = 2E(a'\bar{a}'') - E(^3A'') \quad (10)$$

$$\begin{aligned} E(a - {}^1A') &= \tfrac{1}{2}[E(a'\bar{a}') + E(a''\bar{a}'')] - \sqrt{\Delta^2 + K^2} \\ E(b - {}^1A') &= \tfrac{1}{2}[E(a'\bar{a}') + E(a''\bar{a}'')] + \sqrt{\Delta^2 + K^2} \\ \Delta &= \tfrac{1}{2}[E(a'\bar{a}') - E(a''\bar{a}'')] \\ K &= \tfrac{1}{2}[E(^1A'') - E(^3A'')] \end{aligned} \quad (11)$$

References

1 W.-D. Woggon, *Top. Curr. Chem.*, 1996, **184**, 40.
2 *Cytochrome P-450: Structure, Mechanisms and Biochemistry*, Ed.: P. R. Ortiz de Montellano, Plenum, New York, 1986.
3 M. Sono, M. P. Roach, E. D. Coulter and J. H. Dawson, *Chem. Rev.*, 1996, **96**, 2841.
4 (*a*) J. T. Groves and Y.-Z. Zhang Han, in *Cytochrome P-450: Structure, Mechanisms and Biochemistry*, Ed.: P. R. Ortiz de Montellano, Plenum, New York, ch. 1, 1986; (*b*) J. T. Groves, *J. Chem. Educ.*, 1985, **62**, 928.
5 B. Meunier, *Chem. Rev.*, 1992, **92**, 1411.
6 (*a*) M. Newcomb, M.-H. Le Tadic, D. A. Putt and P. F. Hollenberg, *J. Am. Chem. Soc.*, 1995, **117**, 3312; (*b*) M. Newcomb, M.-H. Le Tadic-Biadatti, D. L. Chestrey, E. S. Roberts and P. F. Hollenberg, *J. Am. Chem. Soc.*, 1995, **117**, 12085; (*c*) P. H. Toy and M. Newcomb, *J. Am. Chem. Soc.*, 1998, **120**, 9718.
7 (*a*) K. A. Lee and W. Nam, *J. Am. Chem. Soc.*, 1997, **119**, 116; (*b*) A. Vaz and J. Coon, *Proc. Natl. Acad. Sci. USA*, 1998, **95**, 3555.
8 (*a*) H.-A. Wagenknecht and W.-D. Woggon, *Chem. Biol.*, 1997, **4**, 367; H.-A. Wagenknecht and W.-D. Woggon, *Angew. Chem.*, *Int. Ed. Engl.*, 1997, **36**, 390; *Angew. Chem.*, 1997, **109**, 404; (*b*) B. Stäubli, H. Fretz, U. Piantini and W.-D. Woggon, *Helv. Chim. Acta*, 1987, **70**, 1173.
9 (*a*) K. Kamaraj and D. Bandyopadhyay, *J. Am. Chem. Soc.*, 1997, **119**, 8099. See especially footnote 13 therein; (*b*) J. T. Groves, Z. Gross and M. K. Stern, *Inorg. Chem.*, 1994, **33**, 5065.
10 D. Schröder and H. Schwarz, *Angew. Chem.*, *Int. Ed. Engl.*, 1995, **34**, 1973.
11 (*a*) W.-D. Woggon, *Nachr. Chem. Tech. Lab.*, 1988, **36**, 890; (*b*) J. H. Dawson, *Science*, 1988, **240**, 433; H. I. Liu, M. Sono, S. Kadkhodyan, L. P. Hager, B. Hedman, K. O. Hodgson and J. H. Dawson, *J. Biol. Chem.*, 1995, **270**, 10544; (*c*) J. Bernardou, A. S. Fabiano, A. Rober and B. Meunier, *J. Am. Chem. Soc.*, 1994, **116**, 9375; (*d*) P. M. Champion, *J. Am. Chem. Soc.*, 1989, **111**, 3434.
12 For pronounced proximal ligand effect on epoxidation in model compounds, see: (*a*) Z. Gross and S. Nimri, *Inorg. Chem.*, 1994, **33**, 1731; (*b*) K. Czarnecki, S. Nimri, Z. Gross, L. M. Proniewicz and J. Kincaid, *J. Am. Chem. Soc.*, 1996, **118**, 2929; (*c*) Z. Gross, *J. Biol. Inorg. Chem.*, 1996, **1**, 368; (*d*) Z. Gross, S. Nimri and L. Simkhovich, *J. Mol. Catal. A: Chem.*, 1996, **113**, 231.
13 (*a*) A. Fiedler, D. Schröder, S. Shaik and H. Schwarz, *J. Am. Chem. Soc.*, 1994, **116**, 10734; (*b*) D. E. Clemmer, Y.-M. Chen, F. A. Khan and P. B. Armentrout, *J. Phys. Chem.*, 1994, **98**, 6522; (*c*) S. Shaik, D. Danovich, A. Fiedler, D. Schröder and H. Schwarz, *Helv. Chim. Acta*, 1995, **78**, 1393; (*d*) K. Yoshizawa, Y. Shiota and T. Yamabe, *J. Am. Chem. Soc.*, 1998, **120**, 564.
14 H. Li, S. Narashimhulu, L. M. Havran, J. D. Winkler and T. L. Poulos, *J. Am. Chem. Soc.*, 1995, **117**, 6297.
15 S. Shaik, M. Filatov, D. Schröder and H. Schwarz, *Chem. Eur. J.*, 1998, **4**, 193.
16 (*a*) For the role of agostic complexes, see: J. P. Collman, A. S. Chien, T. A. Eberspacher and J. I. Brauman, *J. Am. Chem. Soc.*, 1998, **120**, 425; (*b*) for the elucidation of the hydroxylation mechanism in amine oxidation, see: J. P. Dinnocenzo, S. B. Karki and J. P. Jones, *J. Am. Chem. Soc.*, 1993, **115**, 7111; S. B. Karki, J. P. Dinnocenzo, J. P. Jones and K. R. Korezkwa, *J. Am. Chem. Soc.*, 1995, **117**, 3658.
17 (*a*) T. Ziegler, *Chem. Rev.*, 1991, **91**, 651; (*b*) L. A. Eriksson, L. G. M. Petersson, P. E. M. Siegbahn and U. Wahlgren, *J. Chem. Phys.*, 1995, **102**, 872; (*c*) V. Jonas and W. Thiel, *J. Chem. Phys.*, 1995, **102**, 8474 (and references cited therein).
18 (*a*) A. D. Becke, *Phys. Rev. A*, 1988, **38**, 3098; (*b*) J. P. Perdew, *Phys. Rev. B*, 1986, **33**, 8822.
19 R. D. Amos, I. L. Alberts, J. S. Andrews, S. M. Collwell, N. C. Handy, D. Jayatilaka, P. J. Knowles, R. Kobayashi, N. Koga, K. E. Laidig, P. E. Maslen, C. W. Murray, J. E. Rice, J. Sanz, E. D. Simandrias, A. J. Stone and M.-D. Su, *CADPAC5: The Cambridge Analytic Derivatives Package*, Cambridge, UK, 1992.

20 (*a*) H. Kuramochi, L. Noodleman and D. A. Case, *J. Am. Chem. Soc.*, 1997, **119**, 11442; (*b*) A. Ghosh, J. Almløf and L. Que, Jr., *J. Phys. Chem.*, 1994, **98**, 5576.
21 N. Godbout, D. R. Salahub, J. Andzelm and E. Wimmer, *Can. J. Chem.*, 1992, **70**, 560.
22 W. J. Hehre, L. Radom, P. v. R. Schleyer and J. A. Pople, *Ab Initio Molecular Orbital Theory*, Wiley-Interscience, New York, 1986.
23 M. Filatov and W. Thiel, *Mol. Phys.*, 1997, **91**, 847.
24 Computations have been carried out for ferryl-complexes and water-complexes without and with a proximal ligand (NH_3), using FT97 and BP86 with a Wachters basis set on Fe, 6-31G* on O, N (ligand), and N (ring) and STO-3G for C, H (or 6-31G** for H). The basis sets have been abandoned for computer time economy, and FT97 has been waived in favor of the more standard BP86 functional. We note though that these computations gave very similar results to the ones presented in the present paper.
25 (*a*) T. Ziegler, A. Rauk and E. J. Baerends, *Theor. Chim. Acta*, 1977, **43**, 261; (*b*) U. von Barth, *Phys. Rev A*, 1979, **20**, 1693; (*c*) C. Daul, *Int. J. Quantum Chem.*, 1994, **52**, 867.
26 (*a*) A. C. Stückl, C. Daul and H. U. Güdel, *J. Chem. Phys.*, 1997, **107**, 4606; (*b*) K. Doclo, C. Daul and S. Creve, *Int. J. Quantum Chem.*, 1997, **61**, 475; (*c*) F. Giraldoni, J. Weber, K. Bellafrouh, C. Daul and H. U. Güdel, *J. Chem. Phys.*, 1996, **104**, 7624; (*d*) A. C. Stückl, C. Daul and H. U. Güdel, *On the calculation of multiplets*, in *Recent Advances in Density Functional Methods (Part II)*, D. P. Chong, Ed., World Scientific Publishing Co., 1997.
27 C. J. Cramer, F. G. Dulles, D. J. Giesen and J. Almlöf, *Chem. Phys. Lett.*, 1995, **245**, 165.
28 A. A. Ovchinnikov and J. K. Labanowski, *Phys. Rev. A*, 1996, **53**, 3946.
29 U. von Bart, *Phys. Rev. A*, 1979, **20**, 1693.
30 S. Yamamoto, J. Teraoka and H. Kashiwagi, *J. Chem. Phys.*, 1988, **88**, 303.
31 (*a*) G. H. Loew, C. J. Kert, L. M. Hjemeland and R. F. Kirchner, *J. Am. Chem. Soc.*, 1977, **99**, 3534; (*b*) L. K. Hanson, C. K. Chang, M. S. Davis and J. Fajer, *J. Am. Chem. Soc.*, 1981, **103**, 663; (*c*) K. Tatsumi and R. Hoffmann, *Inorg. Chem.*, 1981, **20**, 3771.
32 J. Antony, M. Grodzicki and A. X. Trautwein, *J. Phys. Chem. A*, 1997, **101**, 2692.
33 A. Strich and A. Veillard, *Nouv. J. Chim.*, 1983, **7**, 347.
34 For a Ru analog of type-(II) ferryls, see: J. T. Groves and K. H. Anh, *Inorg. Chem.*, 1987, **23**, 3831.
35 (*a*) G. Loew and M. Dupuis, *J. Am. Chem. Soc.*, 1996, **118**, 10584; (*b*) *ibid.*, 1996, **118**, 10588.
36 The sextet high-spin state ($S = 5/2$) was computed at two different geometries and found to be higher than the states shown in Fig. 8 here. In any event, the energy of the $S = 5/2$ state will not change any of the arguments.
37 H. Thomann, M. Bernardo, D. Goldfrab, P. M. H. Kroneck and V. Ulrich, *J. Am. Chem. Soc.*, 1995, **117**, 8243.
38 (*a*) See also, M. Unno, J. F. Christian, D. E. Benson, N. C. Gerber, S. G. Sligar and P. M. Champion, *J. Am. Chem. Soc.*, 1997, **119**, 6614; (*b*) H. Schappacher, L. Ricard, R. Weiss, E. Bill, R. M. Montoya, H. Winkler and A. X. Trautwein, *Eur. J. Biol.*, 1987, **168**, 419; (*c*) see however, a high-spin with a spatially fixed PhS^- ligand in a fenced prophyrin in ref. 8.
39 J. D. Lipscomb, *Biochemistry*, 1980, **19**, 3590.
40 *Gmelins Handbuch der Anorganischen Chemie. 8. Auflage*, Verlag Chemie, GmbH, Weinheim, 1953.
41 See, M. Filatov and S. Shaik, *J. Chem. Phys.*, 1999, **110**, 116; M. Filatov and S. Shaik, *Chem. Phys. Lett.*, 1998, **288**, 689.
42 R. A. Harman and H. Eyring, *J. Chem. Phys.*, 1942, **10**, 557.
43 M. Filatov and S. Shaik, *J. Phys. Chem. A*, 1998, **102**, 3835.
44 For similar conclusions on the role of thiolate, see: O. Zakharieva, M. Grodzicki, A. X. Trautwein, C. Veeger and I. M. C. M. Rietjens, *J. Biol. Inorg. Chem.*, 1996, **1**, 192.
45 For a discussion of various thiolate ligands and their effect on spectra in Fe^{III} complexes, see: K. K. Stavrev and M. C. Zerner, *Int. J. Quantum. Chem.: Quantum Biol. Symp. 22*, 1995, 155.

Paper 8/09385G